Structural Determinants of P-Glycoprotein-Mediated Transport of Glucocorticoids

Charles R. Yates,[1] Cheng Chang,[2,3] Jeffrey D. Kearbey,[4] Kazuto Yasuda,[5] Erin G. Schuetz,[5] Duane D. Miller,[1] James T. Dalton,[2,4,6] and Peter W. Swaan[2,3,4]

Received March 26, 2003; accepted July 27, 2003

Purpose. The aim of this study was to determine requisite structural features for P-glycoprotein-mediated transport of a series of structurally related glucocorticoids (GCs).

Methods. Transport experiments were conducted in wild-type and stably transfected MDR1 LLC-PK cell line. Transport efficiency ($T_{eff} = P_{eff, B\rightarrow A} / P_{eff, A\rightarrow B}$) in both cell lines was compared as a measure of passive diffusion and P-glycoprotein-mediated transepithelial transport for each steroid. Three-dimensional structure–activity relationships were built to determine how specific structural features within the steroids affect their P-gp–mediated efflux.

Results. Mean (± SD) T_{eff} in LLC-PK cells was 1.1 ± 0.17, indicating that differences in structure and partition coefficient did not affect drug flux in the absence of P-glycoprotein. T_{eff} in L-MDR1 cells ranged from 3.6 to 26.6, demonstrating the importance of glucocorticoid structure to P-glycoprotein transport. The rank order of T_{eff} in MDR1 cells was: methylprednisolone> prednisolone > betamethasone > dexamethasone/prednisone > cortisol. There was no correlation between individual T_{eff} values and partition coefficient. 3D-QSAR models were built using CoMFA and CoMSIA with a q^2 (r^2) of 0.48 (0.99) and 0.41 (0.95), respectively.

Conclusions. Nonpolar bulky substituents around the C-6α position, as well as a hydrogen-bond donor at position C-11, enhance P-glycoprotein affinity and cellular efflux, whereas bulky substituents at C-16 diminish transporter affinity.

KEY WORDS: glucocorticoids; P-glycoprotein; computational biopharmaceutics.

INTRODUCTION

Glucocorticoids, such as methylprednisolone, block the effects of inflammatory cytokines by entering the cell and binding to the intracellular glucocorticoid receptor (GR). It was thought previously that glucocorticoids move freely into and out of the cell by simple diffusion only. However, Meijer and colleagues (1) demonstrated *in vivo* that penetration of dexamethasone into the mouse brain is limited by the presence of mdr1a. Karssen and co-workers (2) demonstrated that P-glycoprotein impairs the penetration of cortisol, but not corticosterone, into the brain of mice and humans. These studies suggest that subtle differences in chemical structure (e.g., absence of a 17α-hydroxyl group) may determine whether a glucocorticoid-like compound will be a substrate for P-glycoprotein. Nakayama and colleagues (3) showed that P-glycoprotein limited the oral absorption of glucocorticoids in a regional-dependent manner (duodenum > jejunum > ileum) with a strong correlation to P-glycoprotein expression along the longitudinal axis of the gastrointestinal tract. Interestingly, the absorption of sex steroids, such as progesterone, was unaltered by the expression of P-glycoprotein. These data corroborate the hypothesis that structural and/or physicochemical properties of individual glucocorticoids determine how efficiently they are transported by P-glycoprotein and that transport by P-glycoprotein plays an important role in determining their *in vivo* efficacy.

In vitro studies demonstrated the ability of P-glycoprotein to limit the transepithelial penetration and, hence, intracellular accumulation of glucocorticoids (4–6). Early studies in this area suggested that glucocorticoid transport efficiency may be related to lipophilicity (7). However, Gruol and Bourgeois (5) demonstrated that various steroid analogues are transported by P-glycoprotein with varying efficiency, based on specific structural recognition sites that mediate P-glycoprotein binding and transport. Gruol and Bourgeois (5) further showed that the number of hydroxyl groups, as well as their position of substitution, affects interaction with P-glycoprotein. For example, steroids lacking both 17- and 21-hydroxy groups are transported much less efficiently than prednisolone, a steroid containing 17- and 21-hydroxyl groups (Fig. 1). Moreover, steroids devoid of hydroxyl groups (e.g., progesterone) are not transported by P-glycoprotein (6,8). Thus, the presence of 11-, 17-, and 21-hydroxyl groups appears to be a critical determinant for transport efficiency of steroids. The current study was designed to investigate the structural elements of glucocorticoids responsible for interaction with P-glycoprotein.

Nonexpressing (LLC-PK) and P-glycoprotein-expressing (L-MDR1) cells were used in transepithelial transport studies of clinically active glucocorticoids to characterize glucocorticoid structural features requisite for P-glycoprotein recognition and transport. The resulting *in vitro* data were used to analyze and correlate structural features of glucocorticoids that contribute to their ability to be recognized and transported by P-glycoprotein. A comprehensive three-dimensional quantitative structure–activity relationship (3D-QSAR) approach was applied using various molecular descriptors. These studies represent the first comprehensive *in vitro* and *in silico* examination of glucocorticoid transport by P-glycoprotein.

METHODS

Chemicals

Cortisol (11α,17β,21-trihydroxypregn-4-ene-3,20-dione), cortisone (4-pregnen-17,21-diol-3,11,20-trione), betamethasone (9α-fluoro-16β-methylprednisolone), prednisone (17α-

[1] Department of Pharmaceutical Sciences, The University of Tennessee, Memphis, TN, 38163.
[2] Biophysics Program, The Ohio State University, Columbus, OH, 43210.
[3] Present address: Department of Pharmaceutical Sciences, University of Maryland, Baltimore MD 21201.
[4] Division of Pharmaceutics, The Ohio State University, Columbus, OH, 43210.
[5] Department of Pharmaceutical Sciences, St. Jude Children's Research Hospital, Memphis, TN, 38105.
[6] To whom correspondence should be addressed. (email: dalton.1@osu.edu)

ABBREVIATIONS: CAL-AM, calcein-AM; CoMFA, comparative molecular field analysis; COMSIA, comparative molecular similarity index analysis; DISCO, distance comparison; L-MDR1, MDR1 transfected LLC-PK.

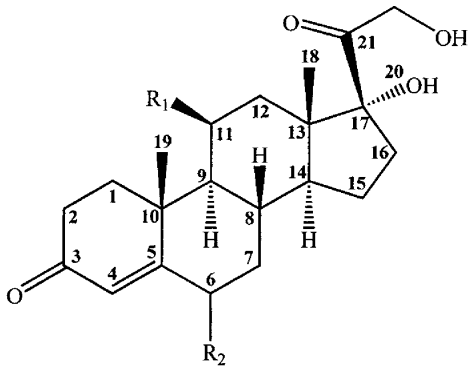

	$-R_1$	$-R_2$
Cortisol	–OH	–H
Cortisone	=O	–H
6α-OH-Cortisol	–OH	····OH
6β-OH-Cortisol	–OH	▬OH

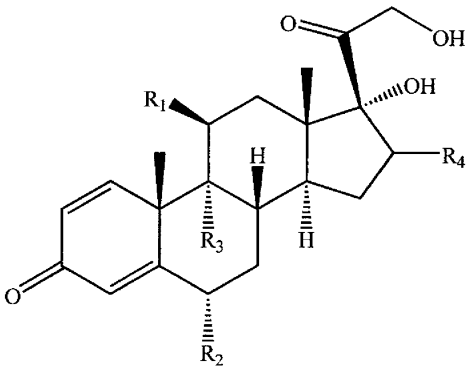

	$-R_1$	$-R_2$	$-R_3$	$-R_4$
Prednisolone	–OH	–H	–H	–H
6-Methylprednisolone	–OH	$-CH_3$	–H	–H
Prednisone	=O	–H	–H	–H
Betamethasone	–OH	–H	–F	▬CH_3
Dexamethasone	–OH	–H	–F	····CH_3

Fig. 1. Chemical structures of glucocortocoid receptor substrates used in this study. Backbone numbering according to IUPAC guidelines. Steroid cyclic rings are named as follows: ring A comprises C1–5,10; ring B, C5–C10; ring C, C8,9,11–14; ring D, C13–17.

21-dihydroxy-1,4-pregnadiene-3,11,20-trione), prednisolone (11β,17α,21-trihydroxy-1,4-pregnadiene-3,20-dione), methylprednisolone (6α-methyl-11β,17α,21-trihydroxy-1,4-pregnadiene-3,20-dione), dexamethasone (9α-fluoro-16α-methylprednisolone), and verapamil were purchased from Sigma (St. Louis, MO). 6α-Hydroxycortisol (4-pregnen-6α,11β,17,21-tetrol-3,20-dione) and 6β-hydroxycortisol (4-pregnen-6β,11β,17,21-tetrol-3,20-dione) were purchased from Steraloids (Newport, RI). Calcein acetoxylmethyl ester (CAL-AM) was obtained from Molecular Probes (Eugene, OR). HPLC-grade acetonitrile was purchased from Fisher Scientific (Fairlawn, NJ). [^{3}H]Dexamethasone was obtained from New England Nuclear (Boston, MA).

Cell Culture

LLC-PK, a pig kidney epithelium–derived cell line, and a variant cell line that stably expresses the product of the human P-glycoprotein gene (L-MDR1) were cultured in Media 199 supplemented with 10% fetal bovine serum, 2 mM L-glutamine, and 100 U/mL penicillin and streptomycin at 37°C in a humidified incubator at 5% CO_2. L-MDR1 cells were cultured with 640 nM vincristine to maintain positive selection of MDR1-overexpressing LLC-PK cells. LLC-PK and L-MDR1 cells were a generous gift of Dr. Alfred Schinkel (The Netherlands Cancer Institute, Amsterdam, The Netherlands). The L-MDR1 variant was characterized previously with respect to extent and specificity of P-glycoprotein overexpression and monolayer growth (9).

The murine macrophage-like cell line J774.2 and an mdr1b overexpressing variant (J774.2 mdr1b) were maintained in DMEM supplemented with 2 mM L-glutamine, 100 U/mL penicillin, 100 μg/mL streptomycin, and 10% heat-inactivated bovine serum. Heat inactivation was achieved by heating serum to 56°C for 30 min. Cells were maintained at 37°C in a humidified incubator at 5% CO_2. The J774.2 mdr1b variant was previously characterized with respect to extent and specificity of P-glycoprotein overexpression (10).

Transwell culture inserts used for transport experiments (3.0-μm pore size, 24.5 mm diameter, microporous polycarbonate membrane; Transwell™ 3414) and all other cell culture supplies were obtained from Costar (Cambridge, MA) or Life Technologies (Rockville, MD).

Determination of MDR Phenotype in LLC-PK and L-MDR1 Cells

Calcein-AM (CAL-AM) is a lipophilic compound that freely passes the cellular membrane. Once inside the cell, the ester moiety is cleaved by ubiquitously expressed intracellular esterases yielding a highly fluorescent metabolite, calcein. CAL-AM is actively extruded by P-glycoprotein. In contrast, calcein, the hydrophilic free acid form, is not a substrate for P-glycoprotein (11). The kinetics of calcein formation can therefore be used to assess functional expression of P-glycoprotein. LLC-PK and L-MDR1 cells (1×10^5) were plated in 96-well plates at a density of 5×10^5 cells/ml in Media 199. After overnight incubation at 37°C, medium was aspirated, and cells were washed with 37°C phosphate-buffered saline (PBS, pH 7.4). CAL-AM (1 μM) was then added, and calcein formation was monitored at 37°C using a Gemini SpectraMax plate reader (Molecular Devices; Sunnyvale, CA) set at excitation and emission wavelengths of 481 nm and 536 nm, respectively. Differences in the rates of calcein formation (dCAL/dt) between LLC-PK and L-MDR1 cells were used to assess expression of functional P-glycoprotein. Parallel experiments were conducted in which CAL-AM (1 μM) was incubated in the absence of cells to account for calcein formation resulting from nonenzymatic ester cleavage. Additional control experiments were conducted to verify that differences in dCAL/dt were related to P-glycoprotein expression. Verapamil (100 μM), a known inhibitor of P-glycoprotein, was added to cells preloaded with CAL-AM (1 μM), and calcein formation was determined as described above. Verapamil is a P-glycoprotein substrate and inhibits transport function without interrupting the catalytic cycle (12).

Transepithelial Transport of Glucocorticoids

Transport experiments were conducted using LLC-PK (control) and L-MDR1 cells. LLC-PK cells form a polarized monolayer permitting bidirectional (basal to apical and apical to basal) assessment of drug flux. In L-MDR1 cells, P-glycoprotein preferentially sorts to the apical membrane enhancing basal to apical flux and inhibiting apical to basal flux. Cells were seeded on microporous polycarbonate membrane filters at a cell density of 2×10^6 cells per well for LLC-PK and L-MDR1 cell lines. The cells were grown for 3 days with daily medium changes. Two hours prior to transport, culture medium was replaced with fresh serum-free medium. For transepithelial transport measurements, the medium on either the basal or apical side was replaced with PBS buffer containing the glucocorticoid of interest (50 μM). The initial donor compartment glucocorticoid concentration (C_0) was selected to achieve detectable receiver compartment concentrations during the linear phase of transport. The cells were incubated at 37°C, and an aliquot (100.0 μl) of buffer from the opposite side of the monolayer (receiver compartment) was withdrawn at 0.5, 1, and 1.5 h.

Parallel experiments were conducted in which the flux for cortisol, prednisolone, and methylprednisolone was determined in the absence of cells. These glucocorticoids were chosen because they represent the range of partition coefficients found in our study. Glucocorticoid (50 μM) was added to the apical well, and an aliquot (100 μl) of buffer from the basal well was withdrawn at 5, 10, and 15 min. Samples were stored at –80°C until HPLC analysis. Each directional transport experiment was conducted in triplicate. Monolayer integrity was verified by measuring transepithelial electrical resistance (TEER) just prior (0 h) to addition of drug and at the end of each transport experiment (1.5 h).

HPLC Assay

An aliquot (100.0 μl) from the receiver compartment was injected onto HPLC (Alliance, Waters Associates; Milford, MA). Standard curves for individual glucocorticoids were constructed and validated over a range of 50 to 2000 ng/ml. The HPLC system consisted of a pump, automated injector (Alliance, Waters Associates), and a photodiode array detector (model 996, Waters Associates). The stationary phase was a Novapak C-18 column protected by a Novapak C-18 precolumn (Waters Associates). The mobile phase consisted of 30% acetonitrile and 70% water and was delivered at a flow rate of 0.9 ml/min. The eluent was monitored at 254 nm. Discrimination between 11-keto and 11-OH glucocorticoids was achieved using a normal phase HPLC assay described elsewhere (13).

Calculation of Effective Permeability Coefficient

Effective permeability coefficients (P_{eff}) were calculated from concentration–time profiles as measured in the receiver compartment according to Fick's first law using the following equation:

$$P_{eff} = \left(\frac{dQ}{dt}\right) \cdot \frac{V}{A \cdot C_0} \quad (1)$$

where dQ/dt represents the appearance of glucocorticoid in the receiver chamber (ng/ml/min), V is the volume of the receiver compartment (cm^3), A is the cross-sectional area, and C_0 is the initial donor concentration (ng/ml) at time = 0. The flux across the monolayer was determined by linear regression from individual glucocorticoid concentration vs. time curves. Comparison of P_{eff} in the basal (B) to apical (A) direction ($P_{eff,\ B\rightarrow A}$) to P_{eff} in the A to B direction ($P_{eff,\ A\rightarrow B}$) in LLC-PK and L-MDR1 cells was used to assess transport efficiency ($T_{eff} = P_{eff,\ B\rightarrow A} / P_{eff,\ A\rightarrow B}$).

Molecular Modeling

Studies were carried on a Silicon Graphics O2 workstation running IRIX 6.5 and SYBYL software suite version 6.7 (Tripos Associates, St. Louis, MO). Where crystal structures were not available, the molecular structures of the substrates were built using standard bond distances and bond angles. Initial minimizations were performed using Tripos force field with a distance-dependent dielectric coefficient and the Powell conjugate gradient algorithm with an energy change convergence criterion of 0.001 kcal/mol. Partial atomic charges (point charges) were calculated with MOPAC (v.6.0) using the AM1 Hamiltonian and the keywords *EF* and *PRECISE*.

DISCO

The DISCO (DIStance COmparisons) module was used to generate pharmacophores for P-glycoprotein-mediated glucocorticoid transport. The method is based on the assumption that the pharmacologic potency of a compound can be represented by its structural points of potential pharmacologic interest, which are named DISCO features, e.g., hydrophobic center or hydrogen bond donor. The pharmacophore is the maximum common features among the set of molecules. Even though glucocorticoids are relatively rigid molecules, a Multisearch routine was run to generate a maximum of 25 conformers for each molecule within 70.0 kcal/mol energy cutoff. Cortisol has the fewest features and conformers of all molecules and was selected as reference compound for the data set (14). DISCO was initially run considering all the potential "feature" points, but additional runs with the specification of a minimum of two hydrophobic centers were executed as well.

CoMFA

CoMFA explains the gradual changes in observed biologic properties by evaluating the electrostatic (Coulombic interactions) and steric (van der Waals interactions) fields at regularly spaced grid points surrounding a set of mutually aligned ligands. Partial Least Square (PLS) was used to correlate the field descriptors with biologic activities. Both fields were calculated using an sp^3 hybridized carbon probe atom (+1 charge at 1.52 Å van der Waals radius) on a 2.0 Å spaced lattice, which extends beyond the dimensions of each structure by 4.0 Å in all directions. A cutoff of 30 kcal/mol ensures that no extreme energy terms will distort the final model. The indicator fields (15) and hydrogen bond fields (16) generated by the "advanced CoMFA" module were also included in the analysis. To eliminate excessive noise, all electrostatic energies below 1.0 kcal/mol and steric energies below 10.0 kcal/mol were set to zero. CoMFA descriptors were used as independent variables, whereas the dependent variable (biologic descriptor) used in these studies was $\log T_{eff}$. Experimental

standard deviations were used as a weighting factor in PLS analyses. The predictive value of the models was evaluated first using Leave-One-Out (LOO) cross-validation. The cross-validated standard coefficient, q^2, was calculated as follows:

$$q^2 = 1 - \frac{\sum_Y (Y_{predicted} - Y_{observed})^2}{\sum_Y (Y_{observed} - Y_{mean})^2} \quad (2)$$

where $Y_{predicted}$, $Y_{observed}$, and Y_{mean} are the predicted, observed, and mean values of the target property (T_{eff}), respectively. $\Sigma(Y_{predicted}-Y_{observed})^2$ is the predictive error sum of squares (PRESS). The standard error of the cross-validated predictions is known as *press*, whereas the root mean squares of the conventional (non-cross-validated) analysis is known as (*s*). The model with the optimum number of PLS components, corresponding to the lowest PRESS value was selected for deriving the final PLS regression models. In addition to the q^2, the conventional correlation coefficient r^2 and its standard error were also calculated. A plot of predicted versus experimental activity was used to identify potential outliers. The process was repeated until no further improvements in q^2 or no outliers could be identified. Results from alternative descriptor fields were compared, and the model with the highest q^2 was accepted. A contour of std* coefficients enclosing the highest 20% value was created for each model.

CoMSIA

Comparative Molecular Similarity Indices Analysis (CoMSIA) differs from CoMFA in that additional hydrogen bond acceptor and hydrophobic fields are calculated (17). Settings (lattice box size, etc.) were identical to those described in CoMFA above. Similarity indices (A_F) for a molecule *j* with atoms *i* at a grid point *q* are calculated as follows:

$$A^q_{F,K}(j) = -\sum_i \omega_{probe,k}\omega_{ik}e^{-ar^2_{iq}} \quad (3)$$

Five physicochemical properties *k* (steric electrostatic, hydrophobic, hydrogen bond donor, and hydrogen bond acceptor) were calculated using a single probe atom. A Gaussian-type distance dependence was used between the grid point *q* and each atom *i* of the molecule using a default attenuation factor (*a*) of 0.3.

RESULTS

Determination of MDR Phenotype in LLC-PK and L-MDR1 Cells

A fluorescence-based microtiter plate assay using CAL-AM was used to confirm the MDR phenotype of LLC-PK and L-MDR1 cells. Differences in the rate of calcein formation (*d*CAL/*d*t) were used to assess P-glycoprotein expression. L-MDR1 cells were incubated in the presence of CAL-AM. Addition of verapamil (100 μM) during CAL-AM treatment resulted in a significant increase in *d*CAL/*d*t (5.3 vs. 1.2 F*/min; $p < 0.001$) in L-MDR1 cells (Fig. 2). As expected, in wild-type LLC-PK cells lacking P-glycoprotein, *d*CAL/*d*t was not significantly affected by verapamil (4.7 vs. 4.6 F*/min; NS), confirming that these cells do not express functional amounts of P-glycoprotein. In L-MDR1 cells, *d*CAL/*d*t in the presence of verapamil was approximately equal to *d*CAL/*d*t in the presence/absence of verapamil in LLC-PK cells, indicating that the differences in *d*CAL/*d*t are attributable to MDR1 expression in L-MDR1 cells. As LLC-PK cells are also devoid of sister of P-glycoprotein (sPGP, also known as "bile salt export pump" (BSEP) or ABC-B11) (18) and multidrug resistance protein (MRP1, ABC-C1) (19), they serve as an excellent model for *in vitro* studies of drug transport and were used for the remainder of our studies.

Transepithelial Transport of Glucocorticoids

Analysis of the transepithelial flux of cortisol in P-glycoprotein transfected LLC-PK cells revealed that the effective permeability in the basolateral to apical direction ($P_{eff,\ B\to A}$) of cortisol was approximately three- to fourfold greater than $P_{eff,\ A\to B}$ (Fig. 3, Table I). In our studies, we used the reciprocal of $P_{eff,\ B\to A}$ over $P_{eff,\ A\to B}$, henceforth named T_{eff}, as a measure of the increase in transport attributed to the P-glycoprotein-mediated component of the overall transepithelial flux (Table I). As expected for P-glycoprotein substrates, control experiments using wild-type LLC-PK cells revealed no significant difference between $P_{eff,\ B\to A}$ and $P_{eff,\ A\to B}$ (i.e., $T_{eff} \simeq 1$; Table I). These data are consistent with previous studies demonstrating P-glycoprotein transport of cortisol (6). All other glucocorticoids tested were substrates for P-glycoprotein as evidenced by a T_{eff} value ranging from 1.8 to 26.6 in L-MDR1 cells (Table I). Mean (± SD) T_{eff} was 1.1 ± 0.17 for all glucocorticoids when their vectorial transport was evaluated in LLC-PK cells (Table I). Prednisolone, which contains two carbon-carbon double bonds in the A-ring, was transported approximately fourfold more efficiently than cortisol, which contains only a single carbon-carbon double bond in the A-ring. The addition of a 6α-methyl substituent to prednisolone (i.e., methylprednisolone) resulted in an increase in T_{eff} of approximately twofold.

Conversely, the addition of 9α-fluoro and 16α/β-methyl groups to prednisolone (i.e., betamethasone and dexamethasone) resulted in a reduction of Teff (± SD) from 12.5 ± 3.5 for prednisolone to 8.3 ± 0.94 and 3.7 ± 0.93 for betamethasone and dexamethasone, respectively (Table I).

In our study, we found no relationship between partition coefficient and T_{eff} (Fig. 4A). However, a negative correlation ($r^2 = 0.84$) between lipophilicity and $P_{eff,\ A\to B}$ was noted when glucocorticoid drug flux was evaluated in LLC-PK cells (Fig. 4B). Significant hydrophobic interaction between glucocorticoids and the polycarbonate membrane of the transwell plate is one possible mechanism to explain these results. However, when P_{eff} values for cortisol, prednisolone, and methylprednisolone were determined in the absence of cells, there was no relationship between partition coefficient and P_{eff} (data not shown). Lipophilic compounds tend to diffuse rapidly across cellular membranes. However, compounds with log octanol water partition coefficients greater than 3.5 exhibit decreased transepithelial permeability coefficients with increasing lipophilicity (20). In addition, it has been proposed that transcellular movement of lipophilic compounds may be restricted owing to interactions with cytoplasmic proteins and partitioning into the intracellular membrane lipid bilayer (21,22). Thus, it is likely that the inverse relationship between permeability and lipophilicity was related to hydro-

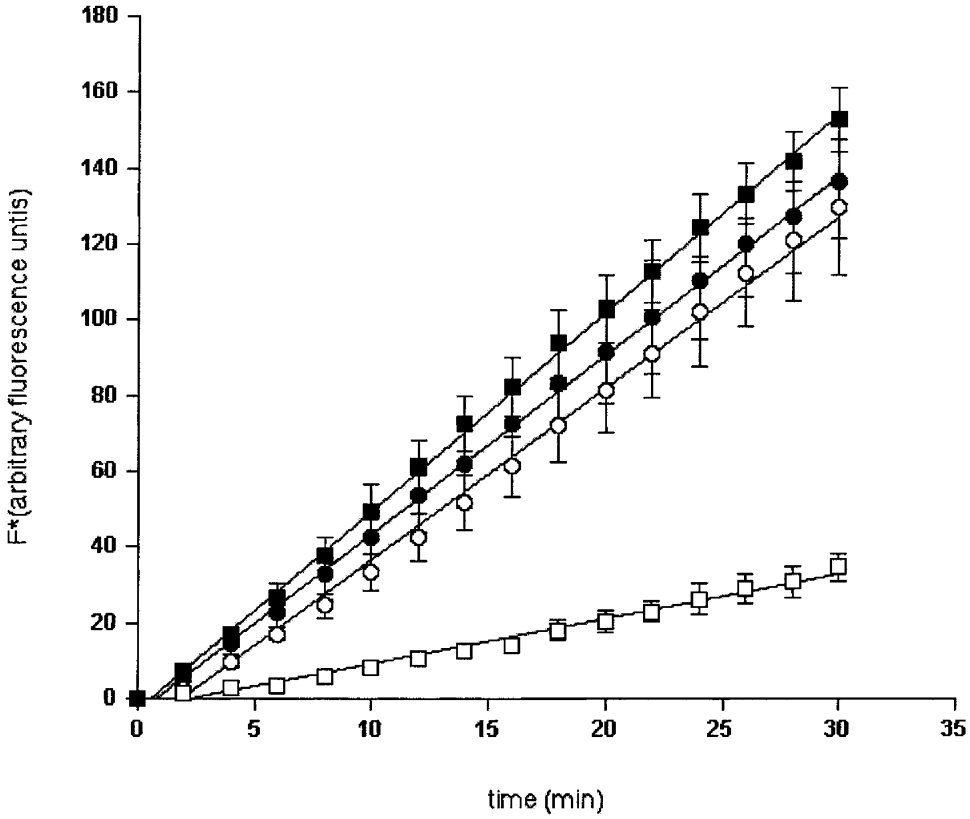

Fig. 2. Calcein formation (*d*CAL/*d*t) in L-MDR1 and LLC-PK cells. *d*CAL/*d*t in the presence (*closed circles*) or absence (*open circles*) of 100 μM verapamil in LLC-PK cells. *d*CAL/*d*t in the presence (*closed squares*) or absence (*open squares*) of 100 μM verapamil in L-MDR1 cells. Data represent mean (± SD) of three independent experiments.

phobic interactions of glucocorticoids with the plasma membrane as well as cytosolic proteins.

Pharmacophore Development

To gain an understanding of the binding mode of glucocorticoid analogues to P-glycoprotein, we used a computational approach to model *in vitro* affinity data. DISCO generated pharmacophore models of the position of important ligand features in three-dimensional space that may ultimately relate to features within P-glycoprotein. These models were derived using multiple conformations of each individual ligand alongside the experimental inhibition data. The result is a computational model that can be used to predict the affinity of glucocorticoids to P-glycoprotein and guide the design of novel glucocorticoid receptor ligands.

A DISCO-generated pharmacophore (Fig. 5) consisted of four hydrophobes, defined as a contiguous set of surface accessible atoms not adjacent to any charge; two hydrogen bond donor sites and two hydrogen bond acceptor atoms. This model has an rms·fit of 0.236 and a union value of 480.6 $Å^3$ (vs. 284.9 for the null hypothesis).

Comparative Molecular Field Analysis

The partial least squares (PLS) algorithm used to derive 3D-QSAR models is a variation of principal component regression in which the original variables are replaced by a small set of linear combinations thereof. The latent variables generated are used for multivariate regression, maximizing the communality of predictor and response variable blocks. The advantage of PLS over other statistical methods is its ability to handle multivariate regression analysis in cases where the number of independent variables is greater than the number of samples. This is particularly useful in CoMFA (and CoMSIA) analyses, where the number of columns, representing the electrostatic and steric values measured by the probe atom at each lattice intersection point is far greater than the number of rows, representing each molecule and its biologic activity data. Overall, PLS reduces the risk of chance correlations (23). Preliminary LOO cross-validated PLS analyses were used to determine the optimum number of components to be used in the final QSAR models. The model depicted in Fig. 6 has a cross-validated r^2 (q^2) of 0.481 with four components and a traditional (non cross-validated) r^2 of predicted versus actual $\log T_{eff}$ of 0.997, as illustrated in Fig. 7A. The residual value of the predicted $\log T_{eff}$ for each individual compound does not exceed 0.04 of its experimental value (Fig. 7B), indicating an internally consistent model. The *press* was 0.394 and *s* was 0.031. The relative contributions of the steric and electrostatic fields were 0.61 and 0.39, respectively.

Comparative Molecular Similarity Index Analysis

The CoMSIA model was derived from identical structural alignments as described for CoMFA. Surprisingly, hydrogen bonding and hydrophobic descriptor fields did not

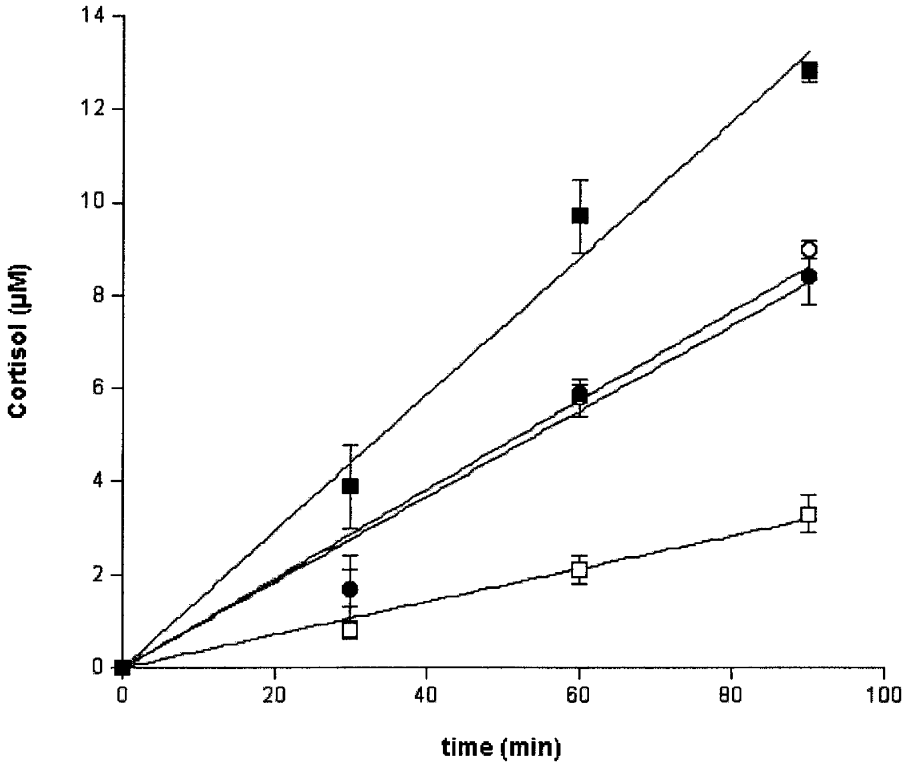

Fig. 3. Transepithelial transport of cortisol. Cortisol flux was measured from the apical to basolateral direction (A-B) (*open symbols*) and basolateral to apical direction (B-A) (*closed symbols*) in LLC-PK (*circles*) and L-MDR1 (*squares*) monolayers on microporous membrane filters. Each time point represents the mean (± SD) of three independent experiments.

contribute significantly to the overall quality of the initial LOO cross-validated models, despite the prevalence of these descriptors in the pharmacophore model. The optimal number of components for a model that included both electrostatic and steric fields was 3 with a q^2 of 0.414 (*press*, 0.374; *s* 0.111), resulting in a conventional r^2 of 0.998. This model (Fig. 6B) corroborates the previously identified steric CoMFA fields (Fig. 6A) but displays more detail in the sterically favored and disfavored areas.

A better ability to visualize and interpret the obtained correlations in terms of field contributions is the major advantage of CoMSIA compared to standard CoMFA. In CoMFA, the steric fields and electrostatic fields are treated simultaneously, and individual field contributions cannot be

Table I. Kinetic Parameters of Glucocorticoid Transepithelial Transport

		LLC-PK		L-MDR1		L-MDR1	LLC-PK
Glucocorticoid	PC	$P_{eff,\ A\to B}$ (±SD)[a]	$P_{eff,\ B\to A}$ (±SD)[a]	$P_{eff,\ B\to A}$ (±SD)[b]	$P_{eff,\ B\to A}$ (±SD)[b]	T_{eff} (±SD)[c]	T_{eff} (±SD)[d]
Betamethasone	87.7[e]	3.7 ± 1.2	4.4 ± 1.3	1.0 ± 0.18	8.0 ± 1.1	8.3 ± 0.94	1.2 ± 0.34
Cortisone	26.2[e]	9.0 ± 0.6	7.4 ± 1.9	5.3 ± 2.0	11.6 ± 3.5	2.3 ± 0.93	1.3 ± 0.25
Cortisol	35.7[e]	6.4 ± 0.5	5.9 ± 0.7	2.2 ± 1.4	7.9 ± 0.67	3.6 ± 0.44	0.92 ± 0.13
6α-OH Cortisol		0.30 ± 0.07	0.34 ± 0.05	0.19 ± 0.07	0.30 ± 0.07	1.8 ± 0.69	1.2 ± 0.49
6β-OH Cortisol		0.76 ± 0.18	0.80 ± 0.12	0.52 ± 0.06	1.2 ± 0.15	2.4 ± 0.44	1.1 ± 0.36
Dexamethasone	67.8[e]	4.5 ± 0.6	4.6 ± 1.5	2.0 ± 0.05	7.3 ± 2.0	3.7 ± 0.93	1.0 ± 0.28
Methylprednisolone	70.7[e]	3.7 ± 0.8	4.0 ± 1.2	0.2 ± 0.4	5.8 ± 0.59	26.6 ± 7.0	1.1 ± 0.29
Prednisone	28.8[f]	8.0 ± 1.0	9.1 ± 1.3	4.2 ± 1.4	14.8 ± 2.3	3.8 ± 1.2	0.89 ± 0.15
Prednisolone	+41.4[e]	6.6 ± 1.8	5.3 ± 1.2	1.0 ± 0.35	12.2 ± 0.5	12.5 ± 3.5	0.80 ± 0.10

[a] Average of $P_{eff,\ B\to A}$ and $P_{eff,\ A\to B}$ determined in LLC-PK cells; $P_{eff,\ A\to B}$, permeability coefficient in the apical (A)-to-basal (B) direction; $P_{eff,\ B\to A}$, permeability coefficient in the B-to-A direction.
[b] Determined in L-MDR1 cells ($\times 10^{-2}$ cm/s).
[c] $T_{eff} = (P_{eff,\ B\to A}/P_{eff,\ A\to B})$ determined in L-MDR1 cells.
[d] $T_{eff} = (P_{eff,\ B\to A}/P_{eff,\ A\to B})$ determined in LLC-PK cells.
[e] PC, partition coefficient (29).
[f] (30).

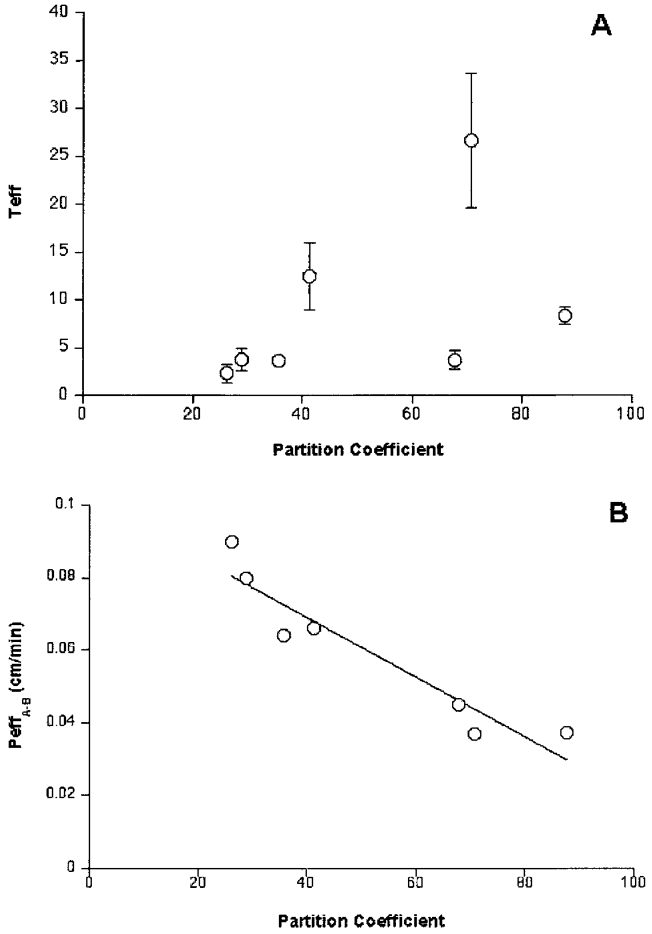

Fig. 4. T_{eff} and P_{eff} versus PC. Transport efficiency (T_{eff}) versus partition coefficient (PC) as determined in L-MDR1 cells (Panel A). Data represent the mean (± SD) of three independent experiments. Plot of permeability (P_{eff}) vs. partition coefficient (PC) as determined in LLC-PK cells (Panel B). Reported P_{eff} values were calculated by averaging P_{eff} values in the apical to basal and basal to apical directions. Data represent the mean of three independent experiments.

revealed. Essentially, the graphs represent isocontours of the obtained coefficients from PLS, indicating those lattice points where a particular property significantly contributes, and thus explain the variation in biologic activity data.

DISCUSSION

Over the past decade, there has been an increasing body of evidence to suggest that glucocorticoid analogues are strates for the efflux transporter P-glycoprotein (1,2,24). thermore, subtle differences in molecular structure appear strongly affect transporter affinity (3,6,8). In the current study, we sought to test the hypothesis that glucocorticoid receptor agonists are P-glycoprotein substrates and to directly correlate P-glycoprotein affinity of glucocorticoid analogues to structural features using *in vitro* transporter assays and molecular modeling approaches.

In the absence of a high-resolution structure for human P-glycoprotein, its structural requirements can be inferred merely by indirect modeling techniques, using variations in molecular structure associated with a change in P-glycoprotein affinity to derive putative transporter-interaction points. However, the complexity of transport by and modulation of P-glycoprotein has been a limiting factor in successful model development. Recently, a study by Ekins and co-workers (25) successfully integrated a structurally diverse data set into a single pharmacophore model for P-glycoprotein affinity. The current study was initiated to expand the P-glycoprotein substrate data set further by determining the structure-activity relationship of a series of glucocorticoid analogues.

In vitro transport studies using transfected cell lines demonstrated that cortisol and prednisolone are better substrates for P-glycoprotein than cortisone and prednisone, respectively, as evidenced by their relative T_{eff} values (Table I). From a structural point of view, our data demonstrate enhanced transport of 11-hydroxyl substituted glucocorticoids as compared to 11-keto glucocorticoids and support prior suggestions by Gruol and Bourgeois (5). Interestingly, prednisone and cortisone, which lack an 11-hydroxyl substituent, are substrates for P-glycoprotein. These data suggest that 11-hydroxyl substitution is not essential for recognition and transport by P-glycoprotein. This conclusion is further supported by control experiments conducted in our laboratory using a normal phase HPLC assay (data not presented) showing that interconversion of 11-hydroxyl and 11-keto steroids (e.g., cortisone conversion to cortisol) did not occur in these cells.

P-glycoprotein recognition and transport of glucocorticoids is affected by other steroid ring substituents. 9α-Fluoro and 16α/β-methyl substitution (i.e., betamethasone and dexamethasone) reduced T_{eff}. Interestingly, 16α-methyl substitution resulted in a greater reduction in T_{eff} compared to 16β-methyl substitution (i.e., dexamethasone T_{eff} was twofold lower than that of betamethasone). These data suggest that P-glycoprotein recognition and transport is sterically hindered by α-orientation of the methyl substitution. Substitution and conformation of the A-ring also affected glucocorticoid recognition and transport. 6α-Methyl substitution (i.e., methylprednisolone) dramatically increased transport whereas 6α/β-hydroxyl substitution (i.e., 6α/β-hydroxycortisol) reduced transport. A hydrophobic pocket within the

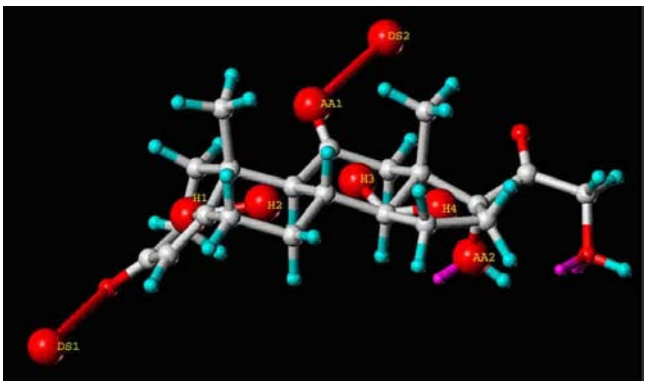

Fig. 5. Pharmacophore model derived from P-glycoprotein-mediated transport efficiency in L-MDR1 cells. The wire frame representation of all individual glucocorticoid analogues used in this study is shown in their overlapping conformations. Pharmacophore feature points (shown by red dummy atoms) are annotated as follows: *AA*, hydrogen bond acceptor atom, *DS*, hydrogen bond donor site; *H*, hydrophobic center. (*This figure appears in color in the online version of this article.*)

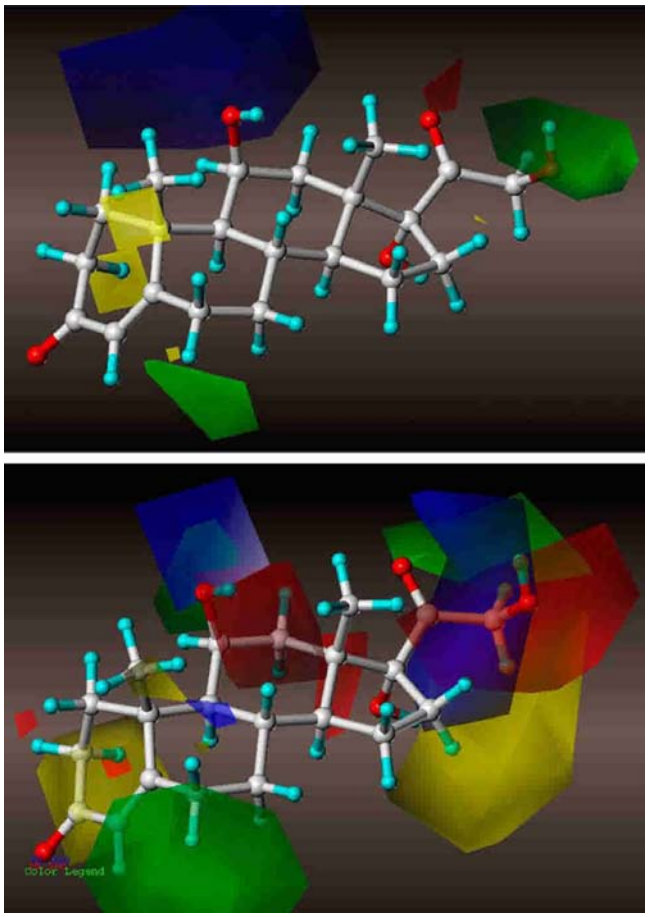

Fig. 6. CoMFA (top) and COMSIA (bottom) models for glucocorticoid analogues. The CoMFA isocontour map of the electrostatic and steric contributions to $\log T_{eff}$ around cortisol shows red contours to indicate regions where negative charge is favorable, whereas blue contours indicate regions where positive charge is favorable. Yellow contours represent regions where steric bulk is unfavorable; green contours indicate areas of the molecules where steric bulk is favorable. Carbon atoms are shown in white, hydrogen atoms in cyan, lone pairs in purple, and oxygen atoms in red. DISCO-derived pharmacophoric feature points are shown as dummy atoms in green. The COMSIA contours illustrate areas where steric bulk is desirable (green) and molecular regions where steric moieties negatively affect $\log T_{eff}$ (yellow). (*This figure appears in color in the online version of this article.*)

steroid recognition site of P-glycoprotein would explain enhanced transport of methylprednisolone and reduced transport of 6α/β-hydroxy cortisol. Lastly, A-ring planarity affects T_{eff} as prednisolone was transported approximately fourfold more efficiently than was cortisol. Taken together, these data demonstrate that structural recognition plays an important role in determining the efficiency with which P-glycoprotein recognizes and transports glucocorticoids.

To further explore the structural characteristics of glucocorticoid affinity to P-glycoprotein, we used a distance constraint pharmacophore building technique as featured in DISCO. Models were built by assessing multiple conformations of each substrate alongside their experimental transport data. DISCO generated four unique pharmacophores that, upon detailed inspection, were essentially similar in that the positioning of hydrogen bond donor sites and hydrogen bond acceptor atoms were interchanged. The consensus model presented in Fig. 5 features four hydrophobic centers, two hydrogen bond donor groups within P-glycoprotein and two hydrogen bond acceptor atoms within the glucocorticoid backbone; interatomic distances between groups are presented in Table II. Because of the limited number of compounds, the pharmacophore essentially emphasizes the essence of the four-ring structure, a 3-keto, 11-hydroxyl (or keto) and 17-α-hydroxyl moieties. Our model for glucocorticoid analogues corresponds very well with the vinblastine transport model recently described by Ekins and colleagues (26), who list four ring aromatic features (hydrophobic centers) and two hydrogen acceptor sites. The advantage of our model is the relative three-dimensional orientation of H-bond donor sites within the protein, which could be useful in determining specific amino acid residues involved in this interaction. A common limitation to pharmacophore models is their failure to report

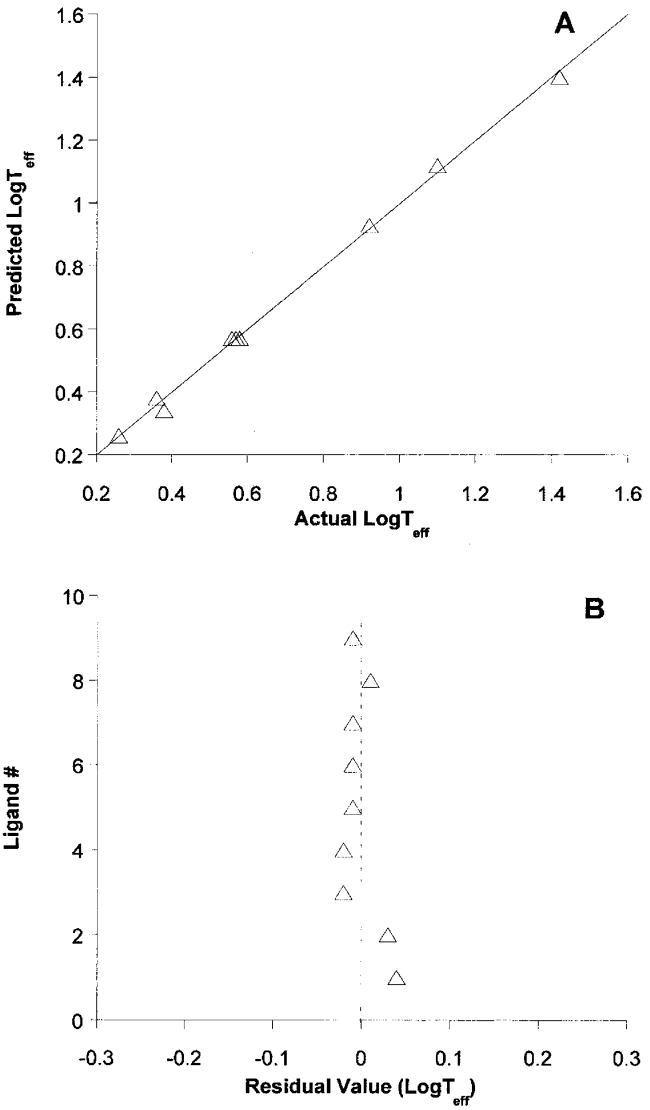

Fig. 7. Experimental versus predicted $\log T_{eff}$ plot of the final CoMFA model for individual glucocorticoid analogues (top). The linear regression line has a slope of 1.0 and an r^2 of 1.00. The individual residuals for all compounds are depicted in the bottom graph.

Table II. Relative Intramolecular Distances Between Pharmacophoric Feature Points (Å)

	Hy_1[a]	Hy_2	Hy_3	Hy_4	DS_1	DS_2	AA_1
Hy-2	2.34						
Hy_3	4.08	2.56					
Hy_4	6.08	4.17	2.26				
DS_1	4.77	6.14	8.38	9.85			
DS_2	6.86	6.5	4.68	5.9	11.6		
AA_1	4.06	3.68	2.55	4.57	8.83	2.9	
AA_2	6.75	5.4	3.3	2.17	9.85	6.05	5.23

[a] AA, acceptor atom; DS, donor site; Hy, hydrophobic center; functional group names correspond to those depicted in Fig. 5.

on steric and electrostatic functionalities that drive short and long range ligand-protein interactions, respectively. Therefore, we extended our model by correlating variability in transport efficiency to variations in molecular structure by implementing 3D-QSAR techniques. Using the molecular overlap from the previously developed pharmacophore model, CoMFA and COMSIA were implemented to inspect the steric, electrostatic and hydrogen bonding fields surrounding the molecules. The resulting models (visualized in Figs. 6A and 6B, respectively) illustrate areas of the molecules where alterations contribute significantly to P-glycoprotein transport. It should be noted that the model was developed using P-glycoprotein *transport* data and therefore, the model reveals molecular regions that contribute to rendering a molecule a P-glycoprotein *substrate*. Both CoMFA and CoMSIA models located a hydrophobic binding pocket around 6-α position indicated by a green contour surrounding this position. It suggests that bulky substituents around the 6-α position can improve the interaction with P-glycoprotein, for example methylprednisolone. These bulky substituents need not to be polar, because no electrostatic contours are drawn in the same area. The yellow contours covering both planes of the A ring in the CoMFA as well as the CoMSIA models (Fig. 5) indicate that less bulky group over or below A ring (i.e. a more planar A ring) would correlate with a better P-glycoprotein transport profile.

The red and blue contours over the 11-hydroxyl group in the CoMSIA model illustrates the importance of both electropositive and electronegative behavior provided by the hydroxyl moiety. CoMFA did not distinguish an electronegative contour (red) in this area, but it shares the electropositive contour over the 11-hydroxyl group. Importantly, this explains why cortisol and prednisolone, bearing a 11-hydroxyl, have higher T_{eff} compared to cortisone and prednisone, which feature a keto group in this position. The CoMSIA model also features a yellow contour over the 16-α position, indicating that bulky substitutions are unfavorable for transportation, as exemplified by the reduced T_{eff} of dexamethasone. Both models display a polar binding pocket at the 17-position, shown by combined green, blue, and red contours. Actually, all glucocorticoids have polar side chains (hydroxyl, keto) at this position. In turn, these observations could be used to specifically design compounds with lower P-glycoprotein affinity and, thus, lead to higher intracellular concentrations.

In vivo studies established the importance of P-glycoprotein in determining tissue penetration of glucocorticoids. For example, Schinkel and colleagues reported increased brain accumulation of dexamethasone, digoxin, and cyclosporin A in mdr1a knockout mice compared to wild-type mice (9). Interestingly, Saitoh *et al.* found that intestinal P-glycoprotein limits the oral absorption of methylprednisolone, but not of cortisol (27). The ability of P-glycoprotein to limit glucocorticoid tissue bioavailability might have important clinical implications as well. Koszdin *et al.* found that P-glycoprotein is responsible for limiting spinal cord bioavailability of methylprednisolone after intravenous administration (28). Thus, limited spinal cord bioavailability of methylprednisolone secondary to P-glycoprotein expression may explain the need for high-level systemic exposure of methylprednisolone in patients with acute spinal cord injury.

As previously suggested, circumvention of P-glycoprotein's effects on steroid activity may be accomplished through development of steroids that do not serve as P-glycoprotein substrates (5). Our group is working on structure-based design of pharmacologically active glucocorticoids that are not transported by P-glycoprotein. In conclusion, our study provides an analysis of glucocorticoid structural features required for recognition by the efflux transporter P-glycoprotein. These data are significant for several reasons. First, these data identify new structural features important in recognition/transport of glucocorticoids (e.g., 6α-substitution). Second, these data provide the framework for studies designed to further elucidate the glucocorticoid recognition site(s) of P-glycoprotein. Third, these data illustrate the potential importance of glucocorticoid selection when targeting tissues with significant P-glycoprotein expression. Overall, our study contributes to the emerging field of P-glycoprotein pharmacophore and 3D-QSAR development that can guide structure-based design of compounds that either target or avoid P-glycoprotein.

ACKNOWLEDGMENTS

Supported in part by grants from Baptist Memorial Healthcare Foundation, the St. Francis of Assisi Foundation of Memphis, and the American Foundation for Pharmaceutical Education (AFPE).

REFERENCES

1. O. C. Meijer, E. C. de Lange, D. D. Breimer, A. G. de Boer, J. O. Workel, and E. R. de Kloet. Penetration of dexamethasone into brain glucocorticoid targets is enhanced in mdr1A P-glycoprotein knockout mice. *Endocrinology* **139**:1789–1793 (1998).
2. A. M. Karssen, O. C. Meijer, I. C. van der Sandt, P. J. Lucassen, E. C. de Lange, A. G. de Boer, and E. R. de Kloet. Multidrug resistance P-glycoprotein hampers the access of cortisol but not of corticosterone to mouse and human brain. *Endocrinology* **142**: 2686–2694 (2001).
3. A. Nakayama, O. Eguchi, M. Hatakeyama, H. Saitoh, and M. Takada. Different absorption behaviors among steroid hormones due to possible interaction with P-glycoprotein in the rat small intestine. *Biol. Pharm. Bull.* **22**:535–538 (1999).
4. S. Bourgeois, D. J. Gruol, R. F. Newby, and F. M. Rajah. Expression of an mdr gene is associated with a new form of resistance to dexamethasone-induced apoptosis. *Mol. Endocrinol.* **7**: 840–851 (1993).
5. D. J. Gruoland S. Bourgeois. Chemosensitizing steroids: glucocorticoid receptor agonists capable of inhibiting P-glycoprotein function. *Cancer Res.* **57**:720–727 (1997).
6. K. Ueda, N. Okamura, M. Hirai, Y. Tanigawara, T. Saeki, N. Kioka, T. Komano, and R. Hori. Human P-glycoprotein transports cortisol, aldosterone, and dexamethasone, but not progesterone. *J. Biol. Chem.* **267**:24248–24252 (1992).

7. C. K. van Kalken, H. J. Broxterman, H. M. Pinedo, N. Feller, H. Dekker, J. Lankelma, and G. Giaccone. Cortisol is transported by the multidrug resistance gene product P-glycoprotein. *Br. J. Cancer* **67**:284–289 (1993).
8. K. M. Barnes, B. Dickstein, G. B. Cutler Jr., T. Fojo, and S. E. Bates. Steroid treatment, accumulation, and antagonism of P-glycoprotein in multidrug-resistant cells. *Biochemistry* **35**:4820–4827 (1996).
9. A. H. Schinkel, E. Wagenaar, L. van Deemter, C. A. Mol, and P. Borst. Absence of the mdr1a P-Glycoprotein in mice affects tissue distribution and pharmacokinetics of dexamethasone, digoxin, and cyclosporin A. *J. Clin. Invest.* **96**:1698–1705 (1995).
10. S. I. Hsu, L. Lothstein, and S. B. Horwitz. Differential overexpression of three mdr gene family members in multidrug-resistant J774.2 mouse cells. Evidence that distinct P-glycoprotein precursors are encoded by unique mdr genes. *J. Biol. Chem.* **264**:12053–12062 (1989).
11. L. Homolya, Z. Hollo, U. A. Germann, I. Pastan, M. M. Gottesman, and B. Sarkadi. Fluorescent cellular indicators are extruded by the multidrug resistance protein. *J. Biol. Chem.* **268**:21493–21496 (1993).
12. J. M. Ford. Experimental reversal of P-glycoprotein-mediated multidrug resistance by pharmacological chemosensitisers. *Eur. J. Cancer* **32A**:991–1001 (1996).
13. C. R. Yates, A. Vysokanov, A. Mukherjee, T. M. Ludden, E. Tolley, G. U. Meduri, and J. T. Dalton. Time-variant increase in methylprednisolone clearance in patients with acute respiratory distress syndrome: a population pharmacokinetic study. *J. Clin. Pharmacol.* **41**:415–424 (2001).
14. Y. C. Martin, M. G. Bures, E. A. Danaher, J. DeLazzer, I. Lico, and P. A. Pavlik. A fast new approach to pharmacophore mapping and its application to dopaminergic and benzodiazepine agonists. *J. Comput. Aided Mol. Des.* **7**:83–102 (1993).
15. R. T. Kroemer, E. Koutsilieri, P. Hecht, K. R. Liedl, P. Riederer, and J. Kornhuber. Quantitative analysis of the structural requirements for blockade of the N-methyl-D-aspartate receptor at the phencyclidine binding site. *J. Med. Chem.* **41**:393–400 (1998).
16. R. S. Bohacek and C. McMartin. Definition and display of steric, hydrophobic, and hydrogen-bonding properties of ligand binding sites in proteins using Lee and Richards accessible surface: validation of a high-resolution graphical tool for drug design. *J. Med. Chem.* **35**:1671–1684 (1992).
17. G. Klebe, U. Abraham, and T. Mietzner. Molecular similarity indices in a comparative analysis (CoMSIA) of drug molecules to correlate and predict their biological activity. *J. Med. Chem.* **37**: 4130–4146 (1994).
18. M. Torok, H. Gutmann, G. Fricker, and J. Drewe. Sister of P-glycoprotein expression in different tissues. *Biochem. Pharmacol.* **57**:833–835 (1999).
19. R. J. Raggers, A. van Helvoort, R. Evers, and G. van Meer. The human multidrug resistance protein MRP1 translocates sphingolipid analogs across the plasma membrane. *J. Cell Sci.* **112**(Pt 3):415–422 (1999).
20. P. Wils, A. Warnery, V. Phung-Ba, S. Legrain, and D. Scherman. High lipophilicity decreases drug transport across intestinal epithelial cells. *J. Pharmacol. Exp. Ther.* **269**:654–658 (1994).
21. G. H. Rothblat and M. C. Phillips. Mechanism of cholesterol efflux from cells. Effects of acceptor structure and concentration. *J. Biol. Chem.* **257**:4775–4782 (1982).
22. B. A. Luxonand R. A. Weisiger. A new method for quantitating intracellular transport: application to the thyroid hormone 3,5,3′-triiodothyronine. *Am. J. Physiol.* **263**:G733–G741 (1992).
23. M. Clarkand R. D. Cramer III. The Probability of Chance Correlation Using Partial Least Squares (PLS). Quant. Struct.-Act. *Relat.* **12**:137–145 (1993).
24. D. J. Gruol, Q. D. Vo, and M. C. Zee. Profound differences in the transport of steroids by two mouse P-glycoproteins. *Biochem. Pharmacol.* **58**:1191–1199 (1999).
25. S. Ekins, R. B. Kim, B. F. Leake, A. H. Dantzig, E. G. Schuetz, L. B. Lan, K. Yasuda, R. L. Shepard, M. A. Winter, J. D. Schuetz, J. H. Wikel, and S. A. Wrighton. Three-dimensional quantitative structure-activity relationships of inhibitors of P-glycoprotein. *Mol. Pharmacol.* **61**:964–973 (2002).
26. S. Ekins, R. B. Kim, B. F. Leake, A. H. Dantzig, E. G. Schuetz, L. B. Lan, K. Yasuda, R. L. Shepard, M. A. Winter, J. D. Schuetz, J. H. Wikel, and S. A. Wrighton. Application of three-dimensional quantitative structure-activity relationships of P-glycoprotein inhibitors and substrates. *Mol. Pharmacol.* **61**:974–981 (2002).
27. H. Saitoh, M. Hatakeyama, O. Eguchi, M. Oda, and M. Takada. Involvement of intestinal P-glycoprotein in the restricted absorption of methylprednisolone from rat small intestine. *J. Pharm. Sci.* **87**:73–75 (1998).
28. K. L. Koszdin, D. D. Shen, and C. M. Bernards. Spinal cord bioavailability of methylprednisolone after intravenous and intrathecal administration: the role of P-glycoprotein. *Anesthesiology* **92**:156–163 (2000).
29. G. L. Flynn. Structural approach to partitioning: Estimation of steroid partition coefficients based upon molecular constitution. *J. Pharm. Sci.* **60**:345–353 (1971).
30. A. Leo, C. Hansch, and D. Elkins. Partition coefficients and their uses. *Chem. Rev.* **71**:525–616 (1971).